



บทความวิจัย

การปรับปรุงประสิทธิภาพของระบบปั๊มน้ำพลังงานแสงอาทิตย์ด้วยตัวควบคุมแบบรบกวนและ สังเกตที่ถูกรับโดยอาศัยหลักการติดตามจุดที่ให้กำลังไฟฟ้าสูงสุด: แบบจำลอง ชุดทดลอง และวิเคราะห์

นฤตล ตีะวรรณภา ฟ้ายัน ตรีกรบุตร และ อภิศักดิ์ เกสุธา

สาขาวิศวกรรมไฟฟ้า คณะวิศวกรรมศาสตร์และเทคโนโลยี มหาวิทยาลัยนอร์ท-เชียงใหม่

รติ วงษ์สถาน* อัจฉรวรรณ เนื่องนิตย์ และ นิลาวรรณ วงศ์ศิลปมรกต

สาขาวิศวกรรมไฟฟ้าและวิศวกรรมคอมพิวเตอร์ คณะวิศวกรรมศาสตร์และเทคโนโลยี มหาวิทยาลัยนอร์ท-เชียงใหม่

* ผู้นิพนธ์ประสานงาน โทรศัพท์ 0 5381 9999 อีเมล: rati@northcm.ac.th DOI: 10.14416/j.kmutnb.2020.12.001

รับเมื่อ 3 ตุลาคม 2562 แก้ไขเมื่อ 6 มีนาคม 2563 ตอรับเมื่อ 23 มีนาคม 2563 เผยแพร่ออนไลน์ 4 ธันวาคม 2563

© 2021 King Mongkut's University of Technology North Bangkok. All Rights Reserved.

บทคัดย่อ

งานวิจัยนี้ได้สร้างแบบจำลองและชุดทดลองอย่างง่ายเพื่อทดสอบประสิทธิภาพของระบบปั๊มน้ำพลังงานแสงอาทิตย์ (Photovoltaic Water Pumping System; PVWPS) ขนาดเล็กที่ไม่ใช้แบตเตอรี่ โดยใช้ตัวควบคุมแบบรบกวนและสังเกตที่ถูกรับ (Modified Perturb and Observe Controller; MP&O) ซึ่งไม่ซับซ้อน และอาศัยหลักการติดตามจุดที่ให้กำลังไฟฟ้าสูงสุด (Maximum Power Point Tracking Method; MPPT) เพื่อเพิ่มประสิทธิภาพการแปลงพลังงานของระบบ (Energy Conversion Efficiency) ซึ่งเป็นอุปสรรคสำคัญในการประยุกต์ใช้เทคโนโลยีพลังงานแสงอาทิตย์สำหรับระบบไฟฟ้ากำลัง ตัวควบคุมที่นำเสนอจะสร้างสัญญาณควบคุมที่มีขนาดขั้นการควบคุมไม่คงที่ให้กับวงจรบัคคอนเวอร์เตอร์ (Buck Converter) เพื่อเลื่อนจุดทำงานไปยังจุดที่ให้กำลังไฟฟ้าสูงสุดของเซลล์แสงอาทิตย์ซึ่งจะถูกส่งผ่านไปยังโหลดคือมอเตอร์และปั๊มน้ำ ระบบ PVWPS-MPPT-MP&O ถูกจำลองโดยใช้โปรแกรม Matlab/Simulink และทวนสอบผลที่ได้จากแบบจำลองด้วยชุดทดลอง ต้นแบบระบบปั๊มน้ำพลังงานแสงอาทิตย์ขนาด 130 วัตต์ ที่ถูกควบคุมผ่านไมโครคอนโทรลเลอร์แบบ Arduino ภายใต้สภาวะจริง ของความเข้มแสงอาทิตย์และอุณหภูมิของแผงเซลล์ที่เปลี่ยนแปลงตลอดวัน ผลการทดสอบพบว่า ตัวควบคุมที่นำเสนอช่วยเพิ่ม ประสิทธิภาพการใช้พลังงาน (Energy Utilization Efficiency) และประสิทธิภาพของเซลล์แสงอาทิตย์ (PV Efficiency) ถึง 75.7 เปอร์เซ็นต์ และ 11.8 เปอร์เซ็นต์ ตามลำดับ ทำให้ประสิทธิภาพรวมของ PVWPS เพิ่มขึ้น 41 เปอร์เซ็นต์ เทียบกับ PVWPS ที่ไม่ใช้ตัวควบคุม

คำสำคัญ: ประสิทธิภาพการใช้พลังงาน การติดตามจุดที่ให้กำลังไฟฟ้าสูงสุด การรบกวนและสังเกตที่มีการปรับเปลี่ยน ระบบ ปั๊มน้ำพลังงานแสงอาทิตย์

การอ้างอิงบทความ: นฤตล ตีะวรรณภา, ฟ้ายัน ตรีกรบุตร, อภิศักดิ์ เกสุธา, รติ วงษ์สถาน, อัจฉรวรรณ เนื่องนิตย์, และ นิลาวรรณ วงศ์ศิลปมรกต, "การปรับปรุงประสิทธิภาพของระบบปั๊มน้ำพลังงานแสงอาทิตย์ด้วยตัวควบคุมแบบรบกวนและสังเกตที่ถูกรับโดยอาศัยหลักการติดตามจุดที่ให้กำลังไฟฟ้าสูงสุด: แบบจำลอง ชุดทดลอง และวิเคราะห์," *วารสารวิชาการพระจอมเกล้าพระนครเหนือ*, ปีที่ 31, ฉบับที่ 1, หน้า 5-15, ม.ค.-มี.ค. 2564.



Improvement Performances of PV Water Pumping System Using MPPT-based Modified P&O Controller: Modeling, Setting Experimental Package and Analysis

Naruedol Tawanna, Falun Takkabutr and Apisak Kesutha

Department of Electrical Engineering, Faculty of Engineering and Technology, North-Chiang Mai University, Chiang Mai, Thailand

Rati Wongsathan*, Atcharawan Nuangnit and Nilawan Wongsinlapamorakot

Department of Electrical and Computer Engineering, Faculty of Engineering and Technology, North-Chiang Mai University, Chiang Mai, Thailand

* Corresponding Author, Tel. 0 5381 9999, E-mail: rati@northcm.ac.th DOI: 10.14416/j.kmutnb.2020.12.001

Received 3 October 2019; Revised 6 March 2020; Accepted 23 March 2020; Published online: 4 December 2020

© 2021 King Mongkut's University of Technology North Bangkok. All Rights Reserved.

Abstract

A very low energy conversion efficiency of the photovoltaic (PV) technology is the main barrier in developing the PV power applications. To address the problem, in this work, a low-cost and simple converter-controller based on the Maximum Power Point Tracking (MPPT) technique is integrated into the small-scale 130-W PV Water Pumping System (PVWPS) without using battery storage. The MPPT-based Modified Perturb and Observe (MP&O) method based on variable step-size control is proposed and demonstrated through Matlab/Simulink software. To validate and verify the simulation model, the MPPT-MP&O is implemented using Arduino microcontroller and applied to the prototype PVWPS. When carried out under the actual weather conditions, as a result, it helps to increase the energy utilization efficiency and the PV efficiency up to 75.7% and 11.8%, respectively, and consequently improves the global efficiency by 41% over the PVWPS without a controller.

Keywords: Energy Utilization Efficiency (EUE), Maximum Power Point Tracking (MPPT), Modified Perturb and Observe (MP&O), Photovoltaic Water Pumping System (PVWPS)

Please cite this article as: N. Tawanna, F. Takkabutr, A. Kesutha, R. Wongsathan, A. Nuangnit, and N. Wongsinlapamorakot, "Improvement performances of PV water pumping system using MPPT-based modified P&O controller: Modeling, setting experimental package and analysis," *The Journal of KMUTNB*, vol. 31, no. 1, pp. 5–15, Jan.–Mar. 2021 (in Thai).

1. Introduction

Nowadays, the photovoltaic (PV) Water Pumping System (WPS) applications are considered as a favorable solution for water supply. However, a high initial cost, about 8 times fossil powered WPS [1], is the disadvantage. Furthermore, the very low global system efficiency usually only varying from 2% to 5% is a major drawback [2]. In addition, the performance of Energy Utilization Efficiency (EUE) is degraded by 23% to 96% at elevated temperatures [3]. To address these problems, the PV sizing optimization for cost-saving [4] and the cooling technique for temperature reduction [5] are applied in most of the PVWPSs, but the total efficiency slightly increases. To optimize the overall efficiency, the PV efficiency that relates directly to the PV power output (PPV) is maximized. However, a PV generator can supply only available power to load, not the maximum power, and the PV characteristics (current-voltage I_{PV} - V_{PV} and P_{PV} - V_{PV} curves) are nonlinear and weather-dependent. Therefore, the maximum power could not be easily detected. To operate at the Maximum Power Point (MPP) that unique on those curves at all times, the controller based on the MPP tracking (MPPT) technique is used ensuring maximum PV efficiency.

In literature, various MPPT algorithms are generally classified as indirect [6], direct [7], and artificial intelligence (AI)-based [8] methods, which are based on off-line analysis depending on the prior knowledge of PV characteristics, online measures of I_{PV} and V_{PV} in determining the MPP, and adaptive control algorithm, respectively. The tradeoff between the non-sensitive to weather changes of the indirect method and the complexity of the

AI-based method, in this work, the direct method is our choice. The Perturb and Observe (P&O) method [7] among the others widely used in the PV systems is chosen due to the ease-of-implementation and low cost because of using only one voltage sensor. On the other hand, the modified P&O (MP&O) methods have been designed to improve the performance of the P&O, e.g. limiting the search space within 70–80% of open-circuit voltage (V_{oc}) [9], determining the voltage at the MPP equals to 77% of V_{oc} [10], and continuously reducing the step-size control from 10% to 0.5% of V_{oc} [11]. However, using those MP&O methods, the system is solely in finding the new V_{oc} that corresponds to the irradiance variations, so that the sun tracker is additionally used, resulting in complexity.

So far, many researchers have actively simulated various P&O methods for the PV systems. However, a few of them implement and analyze those in real practice. In this work, the MPPT-based MP&O based on variable step-size control command is proposed and applied to the PVWPS (Figure 1). First, it is simulated by Matlab/Simulink software. Later, it is implemented by Arduino microcontroller and applied through the converter to the prototype PVWPS. In this work, the small-scale PVWPS (3–25 m³/day) without storage batteries but water tank instead (Figure 1) is considered for optimizing the PVWPS sizing, reducing the cost as well as the regular maintenance, and avoiding the control complexity.

In the test, the performances of the PVWPS with and without controller are evaluated and compared in terms of the efficiencies of individual component, such as dynamic responses, the water

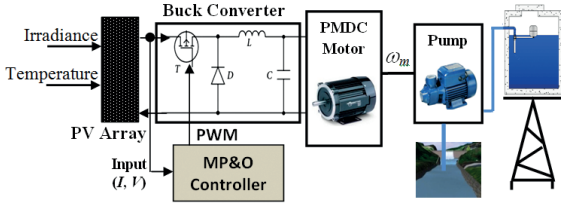


Figure 1 Block diagram of the PVWPS with MP&O-based MPPT controller.

discharge, motor speed, PV efficiency, motor-pump efficiency, global efficiency and EUE. In the following, the description of the PVWPS is described in Section 2) The experimental setting and results are discussed in Section 3) Finally, Section 4) concludes the paper.

2. PVWPS-controller Description

The proposed PVWPS (Figure 1) comprises a PV source, a DC-DC buck converter, an MPPT-MP&O controller in regulating PV voltage, and an electric-powered pump driven by the Permanent Magnet DC (PMDC) motor coupled the centrifugal pump.

2.1 PV modeling and simulation

The equivalent PV-circuit in Figure 2 composed of N_s and N_p connected in series and parallel, respectively, is represented by DC current source, diodes, and series and shunt resistors (R_s and R_{sh}). The nonlinear relationship between I_{PV} and V_{PV} is expressed implicitly relate to the lumped parameters: the photo-current ($I_{ph,0}$), diode saturation current ($I_{sd,0}$), R_s , R_{sh} , and the ideality factor of the diode (A), as shown in Equation (1).

$$I_{PV} = N_p I_{ph} - N_p I_{sd} \left[\exp\left(\frac{qV_{temp}}{AK_B T}\right) - 1 \right] - \frac{V_{temp}}{R_{sh} / N_p}, \quad (1)$$

where $V_{temp} = V_{PV} / N_s + I_{PV} R_s / N_p$, q is the electron

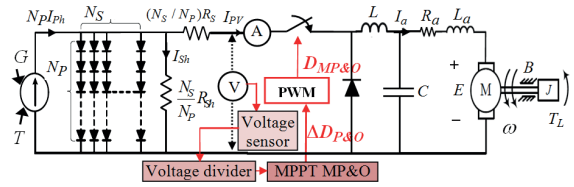


Figure 2 Circuit diagram of the PVWPS with block diagrams of the proposed MPPT-MP&O.

charge, K_B is Boltzmann's constant, and T is the cell temperature (K). The parameter I_{ph} which depends on the irradiance G (W/m^2) and T is given by Equation (2)

$$I_{ph}(G, T) = \left[I_{ph,0} + K_f (T - T_0) \right] \times (G / G_0), \quad (2)$$

where $I_{ph,0}$ is the short circuit current under standard test conditions (STC) of $T_0 = 298$ K and $G_0 = 1000$ W/m^2 , and K_f is the temperature coefficient. The saturated current of diode I_{sd} varied with T can be expressed as to Equation (3).

$$I_{sd}(T) = I_{sd,0} \left(\frac{T}{T_0} \right)^3 \exp \left[\frac{qE_g}{nk_B} \left(\frac{1}{T_0} - \frac{1}{T} \right) \right], \quad (3)$$

where $I_{sd,0}$ is the saturation current under STC, E_g is the band gap energy (eV) of the semiconductor. In the practice, $I_{ph,0}$, $I_{sd,0}$, R_s , R_{sh} , and A , is not provided from manufacturer so that they are evaluated first. To simulate PV characteristics, Equations (1)–(3) are integrated into the Matlab/Simulink (Figure 3).

2.2 DC-DC buck converter design

A buck converter is used to step down V_{PV} to the motor armature voltage (V_a) by the switching duty ratio (D). It is composed of a power switch with the switching frequency f_s , a diode, and an inductor and a capacitor of minimum inductance and capacitance as Equations (4), (5).

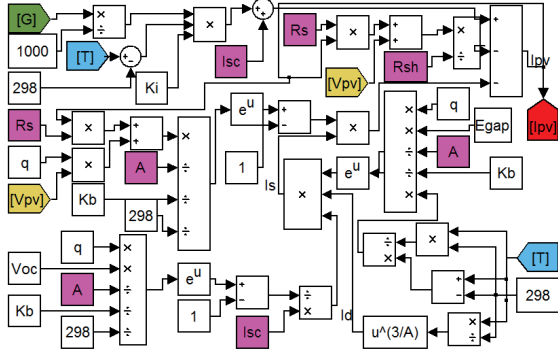


Figure 3 Schematics of the PV module model for generating the I_{PV} - V_{PV} characteristics.

$$L_{min} = \frac{V_a(1-D)}{\Delta I_a f_s}, \quad (4)$$

$$C_{min} = \frac{V_a(1-D)}{8(\Delta V_a) L f_s^2}, \quad (5)$$

respectively, where I_a is armature current, and ΔI_a and ΔV_a are ripple current and voltage, respectively. The output V_a is decreased with respect to the unregulated input V_{PV} as shown in Equation (6).

$$V_a = \eta_{con} D V_{PV} \quad (6)$$

where η_{con} is the buck converter efficiency.

2.3 PMDC motor and pump modeling

To minimize the system, a PMDC motor without requiring a separate field power supply is employed and coupled with the centrifugal pump, which is widely used in PWPS [2]. At steady state, i.e., $d\omega/dt=0$, where ω is the angular speed of motor, the $P_{PV}(G, T)$ delivered to the motor relate to the pump torque, $T_L = K_L \omega^\theta$, is as [3] depicted in Equation (7)

$$P_{PV}(G, T) = \left(\frac{K_L^2 R_a}{K_t^2} \right) \omega^{2\theta} + \left(\frac{2BK_L R_a}{K_t^2} + K_L \right) \omega^{\theta+1} + \left(\frac{B^2 R_a}{K_t^2} + B \right) \omega^2, \quad (7)$$

where R_a is the armature resistance, K_t is the torque constant, B is the damping friction losses, and K_L and θ are the constant parameters of the utilized pump.

The motor-pump efficiency (η_{M-p}), for supplying a flow rate Q (m^3/s) at a Total Dynamic Head (TDH), is

$$\eta_{M-p} = \frac{\rho \times g \times Q \times TDH}{P_{PV}} \times 100, \quad (8)$$

where r is water density, g is gravitational constant. As aforementioned: $TDH = 2$ m, $Q = 0.03$ – 0.6 l/sec, and $P_{PV} = 5$ – 90 W, then η_{M-p} varies between 9–17%. Assuming ideal buck converter (i.e., $\eta_{con} = 100\%$), whereas the PV efficiency is expressed as

$$\eta_{PV} = \frac{P_{PV}}{G \times S_{PV}} \times 100, \quad (9)$$

where S_{PV} is the surface area of PV module. Therefore, the global efficiency is given by

$$\eta_T = \eta_{PV} \eta_{con} \eta_{M-p}, \quad (10)$$

and can increase when η_{PV} or P_{PV} is maximized.

2.4 The MPPT-MP&O method

The typical MPPT-based P&O, i.e., fixed step-size control command, suffers from the oscillations near the MPP at steady-state which deteriorates the performance of the PV system. To address the problem, many works have proposed the improvement of P&O in order to reduce the oscillations but resulting in decreasing the convergence speed. In case of the rapid weather changes, this causes the wrong detection.

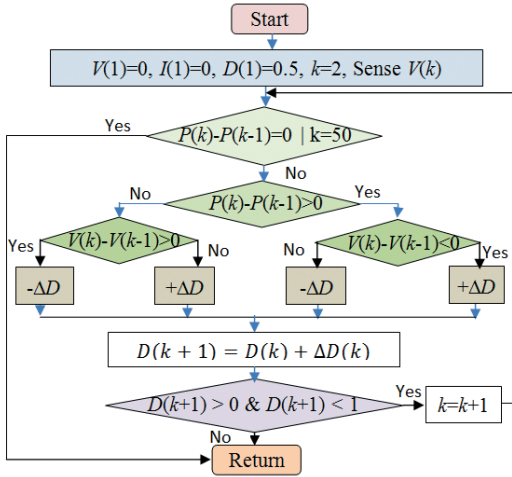


Figure 4 Flow chart of the proposed MP&O controller.

In addition, consider the PV EUE over the time interval $[t_i, t_f]$ which is evaluated by

$$\eta_{utilize} = \int_{t_i}^{t_f} (P_{MP\&O}(t)/P_{MPP}(t)) dt, \quad (11)$$

where $P_{MP\&O}$ is the power obtained from the MP&O method and P_{MPP} is the power at the MPP. The slow tracking in the transient time causes reducing in tracking power then decreases the EUE.

In this work, the MP&O improves the PV performance by using the variable incremental duty ratio, $\Delta D(k)$, instead. It is based on an observation of $P_{PV}(k+1)$ after perturbing on $V_{PV}(k)$ at any operation point (Figure 4). Instead of using the increment or decrement of V_{PV} ($\pm\Delta V_{PV}$) as a controlled output of the MPPT-P&O method which requires the additional PI-controller to regulate the output V_{PV} , to reduce the system complexity, in this work, $\pm\Delta D(k)$ based on the controlled output of the hill climbing MPPT method depending on the movement direction of $\pm\Delta P_{PV}$ is directly used, i.e., $D(k+1) = D(k) \pm \Delta D(k)$, so $\Delta V_{PV}(k+1) = (D(k+1)-1) \times V_{PV}(k)$.

For example, if a given perturbing ΔV_{PV} leads to an increase (decrease) in ΔP_{PV} , the perturbation is generated in that (opposite) direction.

The procedure is repeated until reaching the MPP (slope of $P_{PV}-V_{PV}$ curves in Figure 7(b), $\Delta P_{PV}/\Delta V_{PV} = 0$). Generally, when the MPP is reached, the power oscillates around such the MPP causing wasted energy. The proper step size perturbation helps reduce such the oscillations.

A large step size of the duty ratio helps the rapid convergence to the MPP, but more oscillations are observed at the steady state that results in power loss and heat. On the other hand, a small step size results in lower oscillations but causes a slow tracking leading wrong detection under rapid weather changes. In this work, $\Delta D(k)$ is limited between 0.001 and 1, and the maximum iteration is set to 50. The initial incremental step size is set to be a large value for some first iterations, i.e., $\Delta D(0) - \Delta D(10) = 0.1$, and consequently reduced continuously to the suitable step size for some last iterations.

2.5 PVWPS simulation and implementation

The PVWPS is implemented in Matlab/Simulink (Figure 5) as the masked subsystems: PV-module, buck converter, motor-pump and MPPT-MP&O controller. Whereas, the experimental setup for the small PVWPS, the MP&O controller using Arduino microcontroller, and the actual measures of I_{PV} , V_{PV} , ω and Q are shown in Figure 6.

3. Results and Discussion

For the parameters setup, the 130 W-PV module of polycrystalline silicon commercial (SHARP type

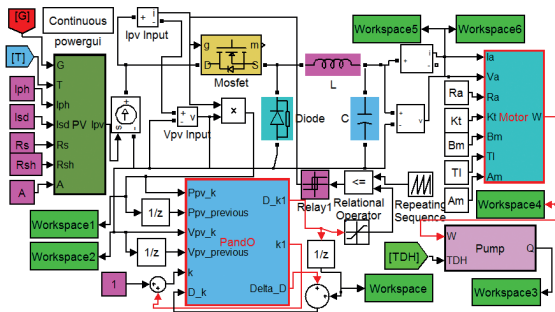


Figure 5 Schematics of the PWPS with converter and the MPPT-MP&O controller.

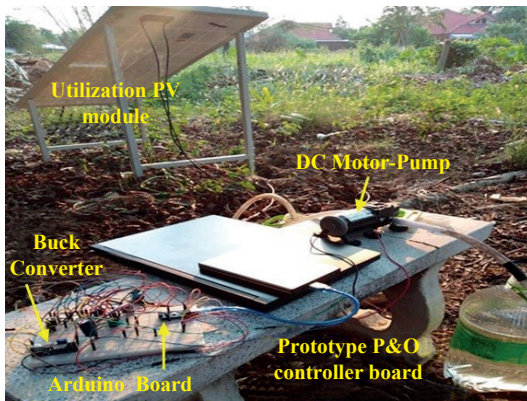


Figure 6 The prototype 130 W-PWPS with the buck converter and MPPT-MP&O controller.

ND-130T1J) composed of 36 cells (N_s) connected in series having $S_{PV} = 0.7 \times 1.50 \text{ m}^2$ is utilized. By the parameter estimation method [12], the lumped PV-parameters are evaluated as: $I_{ph,0} = 8 \text{ A}$, $I_{sd,0} = 8 \mu\text{A}$, $R_s = 16 \text{ m}\Omega$, $R_{sh} = 690 \Omega$, $A = 1.9$, which are substituted into Equations (1)–(3). Under the STC, V_{PV} and I_{PV} at the MPP are 7.48 V and 17.4 V, respectively, and V_{OC} is as 20 V. For the buck converter design, the input PV voltage operates ranging from 5.5 V to 22 V, whereas the output PV voltage to the PMDC motor as load varies from 2 V to 12 V, so that D lies between 0.36–1, Figure 13(e). From Equation (4) and Equation (5), the required

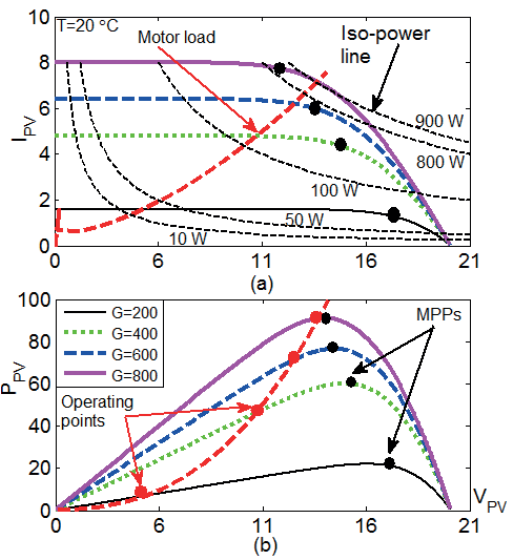


Figure 7 Simulation results of (a) $I_{PV}-V_{PV}$ (b) $P_{PV}-V_{PV}$ against motor load characteristics without controller.

minimum inductance $L_{min} = 614 \mu\text{H} \approx 800 \mu\text{H}$ using Equation (4), and consequently $C_{min} = 0.09 \mu\text{F} \approx 0.5 \mu\text{F}$ using Equation (5), where D_{la} and ΔV_a are assumed to be 5%, and f_s is set as 250 kHz. The parameters of 12 V, 100 W PMDC motor are as follows: $R_a = 2 \Omega$, $B = 2 \times 10^{-6} \text{ Nm}/(\text{rad}/\text{sec})$, and $K_t = 0.067 \text{ N}\cdot\text{m}/\text{A}$. The centrifugal pump has $T_L = 1.67 \times 10^{-6} \omega^{1.8}$. These are substituted in Equation (7) in simulations. Lastly, the proper $\Delta D(k)$ at some last iterations of the P&O method is selected as $\Delta D = 0.015$ by observation from the experiments.

In the test, water source is the well with a TDH of 2 m. The PWPS is carried out under the varying G and T between 200–800 W/m^2 and 35–39°C. The simulation of $I_{PV}-V_{PV}$ and $P_{PV}-V_{PV}$ with motor characteristics is depicted in Figure 7(a), (b), respectively. It is seen that the operating points (red dots) have deviated away from the MPPs (black

dots) so that performance is degraded, especially at low irradiance.

From the simulations in Figure 7(a), it is seen that when the solar irradiance G decreases the PV current falls, whereas the PV voltage slightly increases. For the case of motor-pump load (red dotted line), when the current decreases the voltage also decreases. For instance, with the centrifugal pump, the torque related directly to the current from the PV generator proportionally varies with the square of motor speed. In order to maintain the motor speed, the buck designed buck converter converts the excessive voltage provided from the PV array [Equation (6)] to the additional current.

For the control results under actual weather conditions (Figure 8), the MPPT-MP&O controller provides the operating points (yellow dots) so close the MPP (black, bold line). Thus, the highest possible power is transferred to the motor regardless of the weather variations even under very low irradiance. The convergence to the MPPs using the MPPT-MP&O

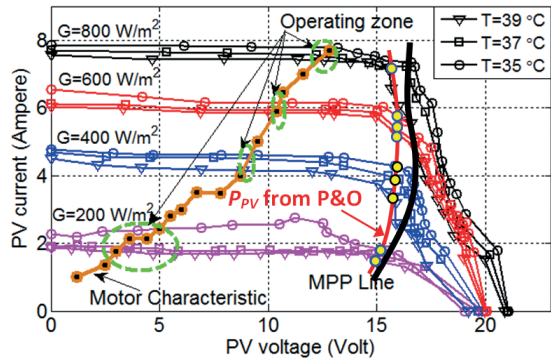


Figure 8 The measured I_{PV} - V_{PV} curves with their corresponding MPPs against the tracked powers by MPPT-P&O.

under the 9 given weather conditions are shown in Figure 9. The main results of the PWWS with and without MPPT-MP&O from the experiments are shown in Figures 10–12.

To compare the PV efficiency between the PWWS with and without the controller, the results for all-weather variations of (G , T) in testing are shown in Figure 10. It is shown in Figure 10(a) that the MPPs increase with the increasing of G and

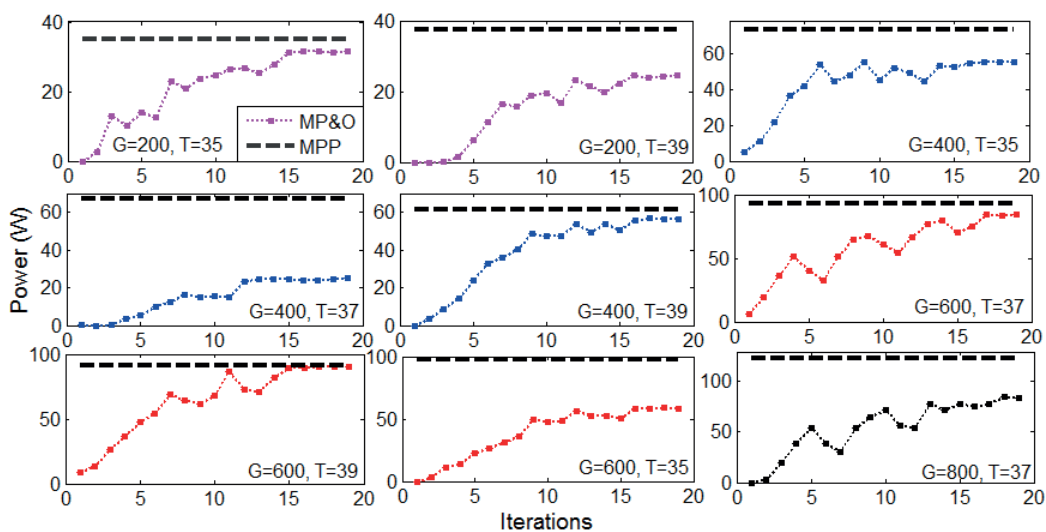


Figure 9 The convergence to the MPPs using the MPPT-MP&O.

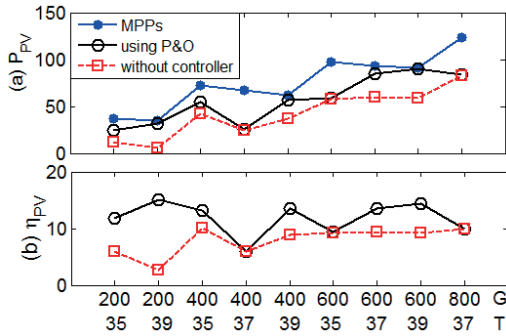


Figure 10 Comparison of PV power P_{PV} and PV efficiency η_{PV} between the PWPS with and without the MP&O controllers under weather variations of (G, T) .

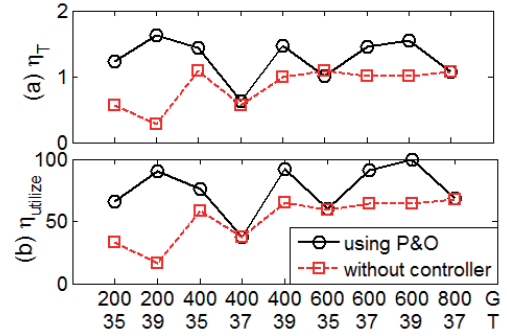


Figure 12 Comparison of total efficiency (η_T) and energy utilization efficiency $(\eta_{utilize})$ between the PWPS with and without the MP&O controllers under weather variations of (G, T) .

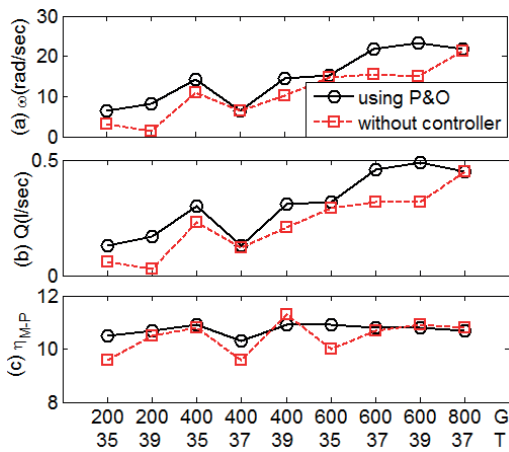


Figure 11 Comparison of water discharge (Q) and motor-pump efficiency (η_{M-P}) between the PWPS with and without the MP&O controllers under weather variations of (G, T) .

decrease when increasing of T which corresponds to the results in Figure 8 (yellow dots on the red line). The system with the proposed MP&O controller achieves the detected power more close to the MPPs than the system without controller for all weather conditions. Consequently, it provides the

average PV efficiency in Equation (9) by 11.85% which is higher than the rest by about 4%, Figure 10(b). However, the proposed MP&O controller performs poorly for some weather conditions, e.g., $G = 400 \text{ W/m}^2$ and $T = 37^\circ\text{C}$, $G = 600 \text{ W/m}^2$ and $T = 35^\circ\text{C}$. It is due to the $I-V$ curves (Figure 8) obtained from the PV panel at such the weather conditions are not smooth and produces many peaks of power near the MPP which are difficult in detecting with the proposed P&O method designed for tracking only one MPP of the uniform weather conditions.

Considering Figure 11(a), (b), it is seen that the flow rate Q increases corresponding to the increasing of the motor speed ω which is directly varied with the current produced by the buck converter. For the low G , the low PV current generating causes low speed and low back emf and consequently reduces the water discharge. However, the motor-pump efficiency in Equation (8) for the PWPS with the proposed MP&O is approximately constant by about 11%. It is also higher than that of the PWPS

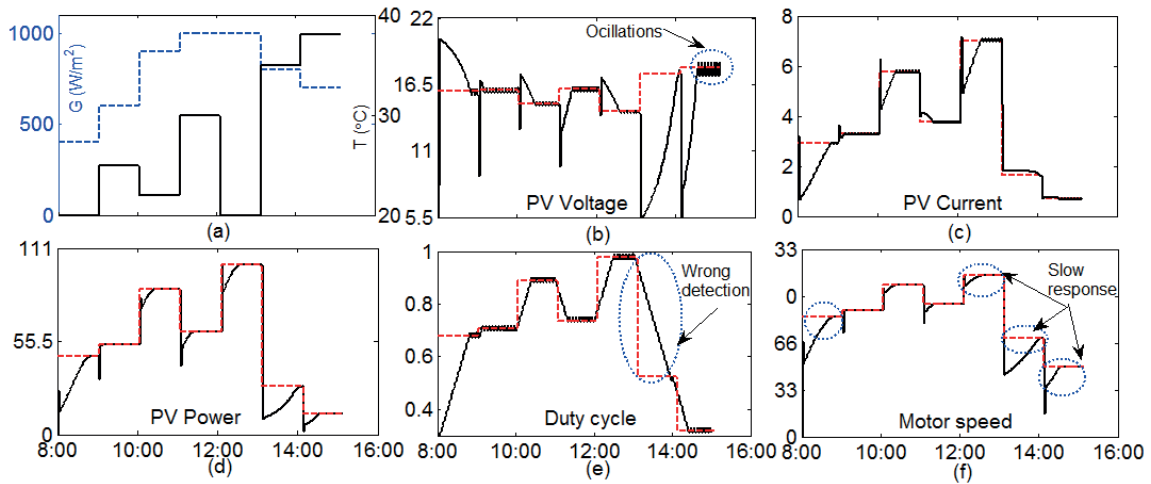


Figure 13 Regulated PV voltage (V_{PV}), PV current (I_{PV}), PV power (P_{PV}), duty ratio (D), and motor speed (ω) of the MPPT-MP&O controller under weather variations.

without the controller for the given constant head, as shown in Figure 11(c).

For the proposed MP&O, the total efficiency in Equation (10) varies between 0.61.6% with an average value of 1.27%, which is improved significantly that of the PVWPS without controller by 37%, as shown in Figure 12(a). From the comparison in Figure 12(b), it averagely provides up to 75.7% EUE Equation (11), which is 31.7% more efficient than the rest.

To investigate the transient and steady-state response of the MPPT-MP&O under fine weather conditions during the daytime in Figure 13, where G and T are varied between 200–1000 W/m^2 , and 20–40°C, respectively, the regulated V_{PV} , P_{PV} , and D , all the cases show the good matching with the optimal values. The good transient response, i.e., small settling time, small rise time, and less overshoot, whereas the good steady-state response, i.e., less oscillation, are observed. However, the control results of the MPPT-MP&O are not satisfied due to slow dynamic response for some weather

conditions, especially at high temperature in the noon. This reduces η_{PV} [Equation (9)] the EUE [Equation (11)] due to the non-optimal P_{PV} and consequently degrades the global efficiency of the PVWPS. In addition, high oscillations occur under some weather conditions that lead to energy losses and heating up to the motor. Moreover, the MPPT-MP&O tracks the MPPs in the wrong direction especially during rapidly changing weather conditions.

4. Conclusions

In this work, improving the PV conversion efficiency of the PVWPS using the efficient MPPT-MP&O controller is our key goal research. The modeling of and prototype PVWPS/MPPT-MP&O are simulated and analyzed by Matlab/Simulink, and implemented through Arduino microcontroller to the prototype PVWPS, respectively. When carried out under weather changes, the efficiencies and dynamic responses are significantly improved over the system without the controller. However, due

to the lack of adaptive control, the slow transient response, wrong tracking direction, and oscillations are considered as inferior. Continuing to develop this work, the AI-based MPPT controllers, such as fuzzy logic and neurofuzzy, are adopted to implement in the PVWPS.

References

- [1] I. Odeh, Y. G. Yohanis, and B. Norton, "Influence of pumping head, insolation and PV array size on PV water pumping system performance," *Solar Energy*, vol. 80, no. 1, pp. 51–64, 2006.
- [2] D. A. Karim and M. M. Marwan, "Solar powered induction motor-driven water pump operating on a desert well, simulation and field tests," *Renewable Energy*, vol. 30, pp. 701–714, 2005.
- [3] I. Seedadan, R. Wongsathan, and A. Nuangnit, "Modeling and simulation of a standalone PV solar-powered water pumping system," presented at the 41st Electrical Engineering Conference (EECon-41), Ubol Ratchathani, Thailand, 2018 (in Thai).
- [4] A. Ksentini, E. Azzag, and A. Bensalem, "Sizing and optimization of a photovoltaic pumping system," *International Journal of Energy Technology and Policy*, vol. 15, no. 1, pp. 71–85, 2019.
- [5] M. Habiballahi, M. Ameri, and S. H. Mansouri, "Efficiency improvement of photovoltaic water pumping system by means of water flow beneath photovoltaic cells surface," *Journal of Solar Energy Engineering*, vol. 137, no. 4, pp. 1–8, 2015.
- [6] T. Anuradha, V. S. Kumar, and P. S. Kumar, "A comparison of existing MPPT techniques for a PV system with interleaved converter," *Australian Journal of Basic and Applied Sciences*, vol. 10, no. 5, pp. 69–75, 2016.
- [7] F. Liu, Y. Kang, Y. Zhang, and S. Duan "Comparison of P&O and hill climbing MPPT methods for grid-connected PV converter," presented at the 3rd IEEE Conference on Industrial Electronics and Applications, Singapore, 2018.
- [8] R. Wongsathan and A. Nuangnit, "Optimal hybrid neuro-fuzzy based controller using MOGA for photo-voltaic (PV) battery charging system," *International Journal of Control Automation and Systems*, vol. 16, no. 6, pp. 3036–3046, 2018.
- [9] M. Kamran, M. Mudassar, M. R. Fazal, M. U. Asghar, M. Bilal, and R. Asghar "Implementation of improved Perturb & Observe MPPT technique with confined search space for standalone photovoltaic system," *Journal of King Saud University - Engineering Sciences*, 2018.
- [10] R. Gammoudi, H. Brahmi, and O. Hasnaoui, "Developed and STM implementation of modified P&O MPPT technique for a PV system over sun," *EPE Journal*, vol. 29, no. 3, pp. 99–119, 2018.
- [11] B. Tan, X. Ke, D. Tang, and S. Yin, "Improved perturb and observation method based on support vector regression," *Energies*, vol. 12, no. 6, pp. 1–11, 2019.
- [12] R. Wongsathan and I. Seedadan, "Artificial intelligence and ANFIS reduced rule for equivalent parameter estimation of PV module on various weather conditions utilized for MPPT," *Journal of Renewable Energy and Smart Grid Technology*, vol. 12, no. 1, pp. 38–55, 2007 (in Thai).